

Real-time forecasting of metro origin-destination matrices with high-order weighted dynamic mode decomposition

Zhanhong Cheng^a, Martin Trépanier^b, Lijun Sun^{a,*}

^a*Department of Civil Engineering, McGill University, Montreal, QC H3A 0C3, Canada*

^b*Department of Mathematics and Industrial Engineering, Polytechnique Montreal, Montreal, QC H3T 1J4, Canada*

Abstract

Forecasting the short-term ridership among origin-destination pairs (OD matrix) of a metro system is crucial in real-time metro operation. However, this problem is notoriously difficult due to the high-dimensional, sparse, noisy, and skewed nature of OD matrices. This paper proposes a High-order Weighted Dynamic Mode Decomposition (HW-DMD) model for short-term metro OD matrices forecasting. DMD uses Singular Value Decomposition (SVD) to extract low-rank approximation from OD data, and a high-order vector autoregression model is estimated on the reduced space for forecasting. To address a practical issue that metro OD matrices cannot be observed in real-time, we use the boarding demand to replace the unavailable OD matrices. Particularly, we consider the time-evolving feature of metro systems and improve the forecast by exponentially reducing the weights for old data. Moreover, we develop a tailored online update algorithm for HW-DMD to update the model coefficients daily without storing historical data or retraining. Experiments on data from a large-scale metro system show the proposed HW-DMD is robust to the noisy and sparse data and significantly outperforms baseline models in forecasting both OD matrices and boarding flow. The online update algorithm also shows consistent accuracy over a long time when maintaining an HW-DMD model at low costs.

Keywords: origin-destination matrices, ridership forecasting, dynamic mode decomposition, public transport systems, high-dimensional time series, time-evolving system

1. Introduction

The metro is a green and efficient travel mode that plays an ever-important role in urban transportation. An accurate real-time ridership/demand forecast is crucial for a metro system's efficiency and reliability. With the wide application of smart card systems and all kinds of sensors, forecasting the real-time metro ridership has become a research hotspot in recent years. Existing research mainly focuses on forecasting the short-term (e.g., 15 or 30 minutes) boarding or alighting ridership at metro stations, such as Wei and Chen (2012); Sun et al. (2015); Li et al. (2017); Chen et al. (2019); Liu et al. (2019b); Zhang et al. (2020b). In contrast, forecasting the short-term ridership at origin-destination (OD) pairs of a metro system receives little attention. The ridership among all OD pairs of a metro system can be organized into a matrix. For simplicity, an "OD matrix" in this paper refers to the ridership of this matrix at a certain (short) time interval.

Forecasting metro OD matrices has much broader applications than the station-level ridership forecast. For example, by assigning OD matrices to a metro network, we can predict and thus regulate each metro train's crowdedness. The station-level boarding/alighting flow also can be calculated from an OD matrix. However, the real-time forecast of metro OD matrices is extremely difficult for the following reasons. (1) The first challenge is the *high dimensionality*. The number of OD pairs of a metro system is squared of the number of stations, often tens of thousands in practice. Moreover, (2) short-term OD matrices of a metro system are *sparse*, and the ridership/flow distribution within an OD matrix is highly *skewed* (Fig. 3). Besides, unlike the boarding or alighting flow, (3) a metro system's OD matrices are not available in real-time (*delayed data availability*). Because an OD matrix can only be obtained after all the trips belonging to the OD matrix have reached their destinations. Lastly, (4) the complex dynamics of a metro system are *time-evolving*; a well-tuned model may have a short "shelf life" and has expensive retrain/re-tune costs in long-term maintenance. Although a few studies tried to forecast the real-time metro OD matrices by matrix

*Corresponding author. Address: 492-817 Sherbrooke Street West, Macdonald Engineering Building, Montreal, Quebec H3A 0C3, Canada

Email addresses: zhanhong.cheng@mail.mcgill.ca (Zhanhong Cheng), mtrepanier@polymtl.ca (Martin Trépanier), lijun.sun@mcgill.ca (Lijun Sun)

factorization methods (Gong et al., 2018, 2020) or deep learning models (Toqué et al., 2016; Zhang et al., 2020a; Shen et al., 2020), no existing solution overcomes all the four challenges above.

To address the above challenges, this paper proposes an effective model for real-time metro OD matrices forecasting. We use the Dynamic Mode Decomposition (DMD) (Schmid, 2010), a recent advance in the fluid flow community, to extract the dominating dynamics from the high-dimensional noisy OD sequence. We extend the original DMD model by a high-order vector autoregression to incorporate long-term temporal correlations. In dealing with the delayed data availability problem, we replace the unavailable latest OD matrices with snapshots of boarding flow. We consider the time-evolving dynamics and introduce a forgetting ratio to reduce the weights of old data exponentially. We name the proposed model High-order Weighted Dynamic Mode Decomposition (HW-DMD). Moreover, we develop a tailored online update algorithm that updates an HW-DMD’s coefficients daily without storing historical data or retraining the model, which greatly reduces the model maintenance costs for long-term implementations. Finally, the proposed model is tested on a Guangzhou metro smart card dataset with 159 stations. Experiments show HW-DMD excellently handles the sparse, skewed, and noise OD data and significantly outperforms baseline models in both the OD matrices and the boarding flow forecast. The online update algorithm also shows consistent accuracy in updating an HW-DMD model over a long period. Hu et al. (2020)

The online HW-DMD model is applied to the metro OD matrices forecast problem, but it can be readily applied to general (high-dimensional) traffic flow forecast problems, such as in recent studies about DMD-based traffic flow forecasting (Avila and Mezić, 2020; Yu et al., 2020). We summary main contributions of this paper as follows:

- This paper proposes an HW-DMD model that addresses various difficulties of the real-time metro OD matrices forecasting. Experiments show the forecast of HW-DMD is significantly better than conventional models.
- The time-evolving dynamics of a transportation system and the maintenance of a forecast model are often ignored in the literature. This paper considers the time-evolving feature of a metro system by reducing the weights for old data and shows improved performance. An online update algorithm is proposed to reduce the long-term maintenance cost of the HW-DMD model under a time-evolving metro system.

The remainder of this paper is organized as follows. We review related work on the short-term OD matrices forecasting in section 2. Next, a formal description of the metro OD matrices forecasting problem is presented in section 3. Section 4 briefly introduces the DMD, which serves as the base for the proposed HW-DMD model. Section 5 is the core part of this paper, where the model specification, estimation method, and the online update method for HW-DMD are elaborated. Section 6 is about the experiments on the Guangzhou metro dataset. Conclusions and future directions are summarized in section 7.

2. Related work

Only a few studies focused on the real-time OD matrices forecasting for a “metro” system. Therefore, we extend the range to general road transportation modes with similar OD matrices forecasting problems, such as the ride-hailing system and the highway tolling system. Note the origins and destinations for a ride-hailing system are often defined on grids.

The matrix/tensor factorization is an effective method to tackle the high-dimensionality problem of OD matrices forecasting. For example, Ren and Xie (2017) applied Canonical Polyadic (CP) decomposition to an *origin* \times *destination* \times *vehicle-type* \times *time* tensor from highway tolling data. Time series models were next built on the latent temporal matrix to forecast OD matrices. Dai et al. (2018); Liu et al. (2020) used principal component analysis (PCA) to reduce the dimensionality of OD data and applied several machine learning models to the reduced data for OD flow forecasting. Gong et al. (2020) developed a matrix factorization model to forecast the OD matrices of a metro system. Their work highlights a solution to the delayed data availability problem and various spatial and temporal regularization that improves the forecast. Concisely, the matrix/tensor factorization-based OD matrices forecasting includes two parts: 1) a dimensionality reduction by the factorization and 2) a forecasting model applied to the reduced data. Usually, using regularization techniques can improve the forecast.

Deep-learning is another mainstream method for OD matrices forecasting. In an early study, Toqué et al. (2016) used Long Short Term Memory (LSTM) networks to forecast the OD matrices of a transit network. They only applied the model to selected high-flow OD pairs because of the high dimensionality problem. Convolutional Neural Networks (CNN) and Graph Convolutional Networks (GNN) are two deep-learning models that greatly reduce the model size compared with a fully connected neural network. Recently, using CNN/GCN to capture spatial correlations and LSTM to capture temporal correlations started to become the “standard configuration” for deep-learning-based OD matrices forecasting. For example, Chu et al. (2019) used multi-scale convolutional LSTM to forecast the real-time taxi OD demand, Wang et al. (2019b, 2020) used multi-task learning to improve the OD flow forecast of GCN+LSTM

networks. A large body of literature focused on better utilizing the spatial/semantic correlations by optimizing the GNN structure or incorporating side information. Such as the local spatial context used by Liu et al. (2019a), the Spatio-Temporal Encoder-Decoder Residual Multi-Graph Convolutional network (ST-ED-RMGC) proposed by Ke et al. (2021), and the Dynamic Node-Edge Attention Network (DNEAT) developed by Zhang et al. (2021). Some studies combined deep-learning models with other models to complement each other. In this direction, (Xiong et al., 2020) combined GCN with Kalman filter to forecast the OD matrices of a Turnpike network. Shen et al. (2020) mixed CNN with a Gravity model to forecast OD matrices of a metro system. Hu et al. (2020) considered the travel time between OD pairs as a stochastic variable, and developed a stochastic OD matrices forecasting model based on tensors factorization and GCN.

The effect of deep-learning models is often impaired by the noise in sparse metro OD matrices. To reduce the impact of noise, Zhang et al. (2019b, 2020a) developed a metric called OD attraction degree (ODAD) to mask the insignificant OD pairs. Zhang et al. (2019b) showed masking near-zero OD pairs improves the forecasting of an LSTM. Based on ODAD, Zhang et al. (2020a) developed a Channel-wise Attentive Split-CNN (CAS-CNN) model for metro OD matrices forecasting. Another merit for this work is they considered the delayed data availability problem.

In summary, matrix/tensor factorization, CNN, and GCN all aim to reduce model size while maintaining spatial/temporal correlations. The HW-DMD model proposed in this paper belongs to the matrix factorization category. Although some ride-hailing systems may not have the delayed data availability problem; most research essentially omitted this problem for simplicity. Particularly, RNN-based deep-learning models can barely work without the latest OD matrices as inputs. In dealing with the delayed data availability problem, existing solutions (Gong et al., 2020; Zhang et al., 2020a; Xiong et al., 2020) used alternative quantities (e.g., boarding ridership, link flow) to compensate for the unavailable OD information. This paper also adopts this approach.

3. Problem Description

Many modern metro systems record passengers’ entry and exit information. We thus know the origin and destination stations, the start and end time for every trip in such a system. Given a fixed time interval (30 minutes in this paper), we denote $o_{t,i,j}$ to be the number of trips that depart from station i at the t -th interval to station j . We call $o_{t,i,j}$ an *OD flow*. Next, we can describe the number of trips between every OD pair in the system at the t -th time interval by an *OD matrix*

$$O_t = \begin{bmatrix} o_{t,1,1} & \cdots & o_{t,1,s} \\ \vdots & \ddots & \vdots \\ o_{t,s,1} & \cdots & o_{t,s,s} \end{bmatrix} \in \mathbb{R}^{s \times s}, \quad (1)$$

where s is the number of metro stations. The diagonal elements of a metro OD matrices are always zero. We keep these zero elements because they have a negligible effect on the forecast. In our model, OD matrices are organized in a vector form

$$\mathbf{f}_t = \text{vec}(O_t) = [o_{t,1,1}, \cdots, o_{t,s,1}, o_{t,1,2}, \cdots, o_{t,s,2}, \cdots, o_{t,1,s}, \cdots, o_{t,s,s}]^\top \in \mathbb{R}^n, \quad (2)$$

where $n = s \times s$ is the number of OD pairs. For convenience, we refer to \mathbf{f}_t as an *OD snapshot*.

Note OD snapshots are aggregated by the time when passengers enter the system; the exit time might be in a different time interval. Therefore, an OD snapshot for interval t can only be obtained after all the passengers entered at interval t have reached their destinations; it cannot be observed in real-time (i.e., the delayed data availability). In contrast, the boarding (entering) flow—another important quantity—is real-time observable. We denote $b_{t,i}$ as the number of passengers entering station i at interval t . In fact, there is $b_{t,i} = \sum_j o_{t,i,j}$. We define a *boarding snapshot* as a vector $\mathbf{b}_t = [b_{t,1}, b_{t,2}, \cdots, b_{t,s}]^\top$.

The OD matrices/flow forecasting problem is to forecast future OD snapshots $\mathbf{f}_{t+1}, \mathbf{f}_{t+2}, \cdots, \mathbf{f}_{t+L}$ given a sequence of historical OD snapshots $\mathbf{f}_1, \mathbf{f}_2, \cdots, \mathbf{f}_t$ and boarding snapshots $\mathbf{b}_1, \mathbf{b}_2, \cdots, \mathbf{b}_t$. The reason for using boarding snapshots is to compensate for the delayed data availability problem of recent OD snapshots.

4. Dynamic Mode Decomposition

Dynamic Mode Decomposition (DMD, Schmid, 2010) was developed in the fluid dynamic community to extract dynamic features from high-dimensional data. To better illustrate our forecast model, we briefly introduce DMD in this section.

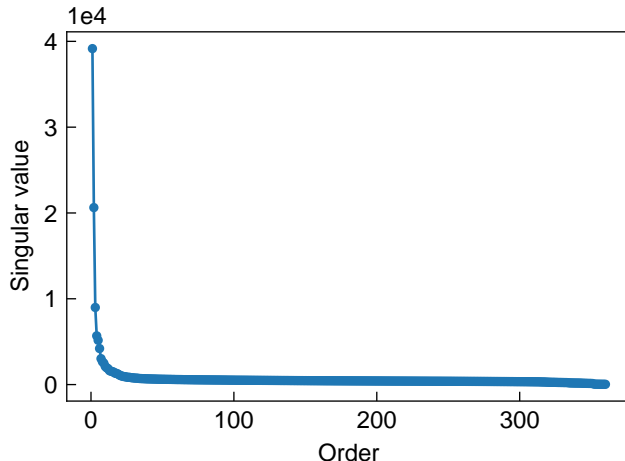


Figure 1: The singular values of a ten-day-length Y_{t-1} collected from Guangzhou metro smart card system.

Consider using a linear dynamical system $\mathbf{f}_i \approx A\mathbf{f}_{i-1}$ for OD flow forecasting. Similar to many fluid problems, n is huge for an OD snapshot and even storing $A \in \mathbb{R}^{n \times n}$ can be prohibitive. Therefore, DMD outputs the (leading) eigenvalues and eigenvectors of A without calculating the expensive A . The eigenvectors of A are referred to as the DMD modes and have clear physical meaning. Each DMD mode is associated with an oscillation frequency and a decay/growth rate determined by its eigenvalue. DMD is also connected to Koopman theory and can model complex non-linear systems by constructing proper measurements (Rowley et al., 2009). There are many variant algorithms for DMD. We only present the *exact DMD* (Tu et al., 2014), which is closely related to this paper.

We arrange OD snapshots into m -column matrices $Y_i = [\mathbf{f}_{i-m+1}, \mathbf{f}_{i-m+2}, \dots, \mathbf{f}_i] \in \mathbb{R}^{n \times m}$. Typically, $m \ll n$. The linear dynamical system follows $Y_t \approx AY_{t-1}$. The exact DMD seeks the leading eigenvalues and eigenvectors of the best-fit linear operator A by the following procedure.

1. Compute the truncated singular value decomposition (SVD) $Y_{t-1} = U\Sigma V^\top$, where $U \in \mathbb{R}^{n \times r}$, $\Sigma \in \mathbb{R}^{r \times r}$, and $V \in \mathbb{R}^{m \times r}$ and $r \ll m$.
2. Instead of computing the full matrix $A = Y_t Y_{t-1}^+ \approx Y_t V \Sigma^{-1} U^\top$.¹ We define a reduced matrix $\tilde{A} = U^\top A U \approx U^\top Y_t V \Sigma^{-1} \in \mathbb{R}^{r \times r}$. It can be proved that \tilde{A} and A have the same nonzero leading eigenvalues (Tu et al., 2014).
3. Compute the eigenvalue decomposition $\tilde{A}W = W\Lambda$. The entries of the diagonal matrix Λ are also the eigenvalues of the full matrix A .
4. The DMD modes (eigenvectors of A) can be obtained by $\Phi = Y_t V \Sigma^{-1} W$.

Fig. 1 shows the singular values of a ten-day-length Y_{t-1} from smart card data of the Guangzhou metro system. A few leading singular values explain a significant portion of the variance, showing the low-rank feature of OD snapshots data. DMD-based model can thus greatly reduce the dimensionality/complexity of such a dynamic system. However, the exact DMD has some limitations for the OD flow forecasting problem. Firstly, the complex temporal correlation of OD flow cannot be well captured by a linear dynamical system. Moreover, using the last OD snapshot is impractical since OD snapshots cannot be observed in real-time. To address these problems, we propose our solution in the next section.

5. High-order Weighted Dynamic Mode Decomposition

5.1. Model Specification

The forecasting formula of an exact DMD amounts to a high-dimensional 1-order vector autoregression. However, the latest OD snapshots are unknown at the time of forecasting. Therefore, we use the two latest snapshots of the

¹ $(\cdot)^+$ denotes the Moore–Penrose inverse of a matrix.

boarding flow as a replacement. We regard OD snapshots of three or more intervals ago as available; because we find more than 96% trips in our dataset are completed within one hour (two lags). And we can use a high-order vector autoregression to capture the long-term correlations in OD snapshots. The forecasting model follows

$$\mathbf{f}_i \approx A_{t,1}\mathbf{f}_{i-q_1} + A_{t,2}\mathbf{f}_{i-q_2} + \cdots + A_{t,h}\mathbf{f}_{i-q_h} + A_{t,b1}\mathbf{b}_{i-1} + A_{t,b2}\mathbf{b}_{i-2} \quad \forall i \in \{q_h + 1, q_h + 2, \dots, t\}. \quad (3)$$

Where time lags for OD snapshots are positive integers satisfying $3 \leq q_1 < \cdots < q_h < t$. Note that coefficient matrices $A_{t,1}, \dots, A_{t,h} \in \mathbb{R}^{n \times n}$ and $A_{t,b1}, A_{t,b2} \in \mathbb{R}^{n \times s}$ are estimated using the data up to the latest (t -th) time interval; they are re-estimated when new data become available. This allows the model's coefficients to be time-varying. We will introduce how to update coefficient matrices using new observations without storing historical data in section 5.3. Note this same model framework can be easily extended to incorporate higher-order boarding flow or other external covariates (e.g. alighting flow, historical average flow). This paper only presents the model in Eq. (3) as an example.

To express Eq. (3) in a concise matrix form. Let $Y_i = [\mathbf{f}_{i-m+1}, \mathbf{f}_{i-m+2}, \dots, \mathbf{f}_i]$ and $B_i = [\mathbf{b}_{i-m+1}, \mathbf{b}_{i-m+2}, \dots, \mathbf{b}_i]$, where $m = t - q_h$ is the number of target snapshots. Then, Eq. (3) is equivalent to

$$Y_t \approx A_{t,1}Y_{t-q_1} + A_{t,2}Y_{t-q_2} + \cdots + A_{t,h}Y_{t-q_h} + A_{t,b1}B_{t-1} + A_{t,b2}B_{t-2} \quad (4)$$

$$= [A_{t,1}, A_{t,2}, \dots, A_{t,h}, A_{t,b1}, A_{t,b2}] \begin{bmatrix} Y_{t-q_1} \\ Y_{t-q_2} \\ \vdots \\ Y_{t-q_h} \\ B_{t-1} \\ B_{t-2} \end{bmatrix} \quad (5)$$

$$= G_t X_t, \quad (6)$$

where $G_t \in \mathbb{R}^{n \times (hn+2s)}$ and $X_t \in \mathbb{R}^{(hn+2s) \times m}$ are augmented matrices for coefficients and data, respectively.

The system's dynamics may change over time. Therefore, we introduce a forgetting ratio ρ that assigns smaller weights on snapshots in older days. The matrix G_t can be solved by an optimization problem

$$\min_{G_t} \sum_{i=1}^m \rho^{\text{day}(m) - \text{day}(i)} \|\mathbf{y}_i - G_t \mathbf{x}_i\|_F^2 \quad 0 < \rho \leq 1. \quad (7)$$

Where \mathbf{y}_i and \mathbf{x}_i are the i -th column of Y_t and X_t , respectively; $\text{day}(i)$ represents the day of the snapshot \mathbf{y}_i . We assign the same weight for snapshots of the same day. The weight $\rho^{\text{day}(m) - \text{day}(m)} = \rho^0 = 1$ for the latest OD snapshot. For a snapshot in j day ago, the weight is ρ^j , which decreases exponentially. This weighting idea is similar to works by [Alfatlawi and Srivastava \(2019\)](#); [Zhang et al. \(2019a\)](#); [Kwak and Geroliminis \(2020\)](#). For convenience, we define $\sigma = \sqrt{\rho}$ and the weighted version of Y_t and X_t as

$$Y_t^w = [\sigma^{\text{day}(m) - \text{day}(1)} \mathbf{y}_1, \sigma^{\text{day}(m) - \text{day}(2)} \mathbf{y}_2, \dots, \mathbf{y}_m] \quad (8)$$

$$X_t^w = [\sigma^{\text{day}(m) - \text{day}(1)} \mathbf{x}_1, \sigma^{\text{day}(m) - \text{day}(2)} \mathbf{x}_2, \dots, \mathbf{x}_m]. \quad (9)$$

Then, the optimization problem in Eq. (7) becomes an ordinary least squares problem

$$\min_{G_t} \|Y_t^w - G_t X_t^w\|_F^2. \quad (10)$$

We summary our higher-order weighted DMD (HW-DMD) framework by Fig. (2). The underlying forecasting model is a high-order vector autoregression with the boarding flow as extra inputs. A forgetting ratio is introduced to decrease the weights of old data exponentially in a daily basis. In section 5.2, we will introduce a dimensionality reduction technique based on DMD to find a low-rank solution for this tremendous model. Instead of full matrices $A_{t,(\cdot)}$, we seek $\tilde{A}_{t,(\cdot)}$ —much smaller matrices—to capture the system's dynamic. Finally, an online update method is proposed in section 5.3 to update the model coefficients incrementally without storing historical data. This provides a memory-saving solution that maintains an up to date model.

The proposed HW-DMD is closely related to Hankel-DMD ([Brunton et al., 2017](#); [Arbabi and Mezić, 2017](#); [Avila and Mezić, 2020](#)) and DMD with control (DMDc, [Proctor et al., 2016](#)). Hankel-DMD uses Hankel data matrices as input and output to model a non-linear dynamical system by a linear model; its DMD modes approximate to Koopman modes. Instead, HW-DMD uses raw snapshots as the output (the left side of Eq. (4)) without the Hankel structure. It is neater and more suitable in the context of forecasting. Besides, our model can use non-continuous orders and external variables (e.g., the boarding flow). Essentially, the external variable of our model is similar to the control term of a DMDc model.

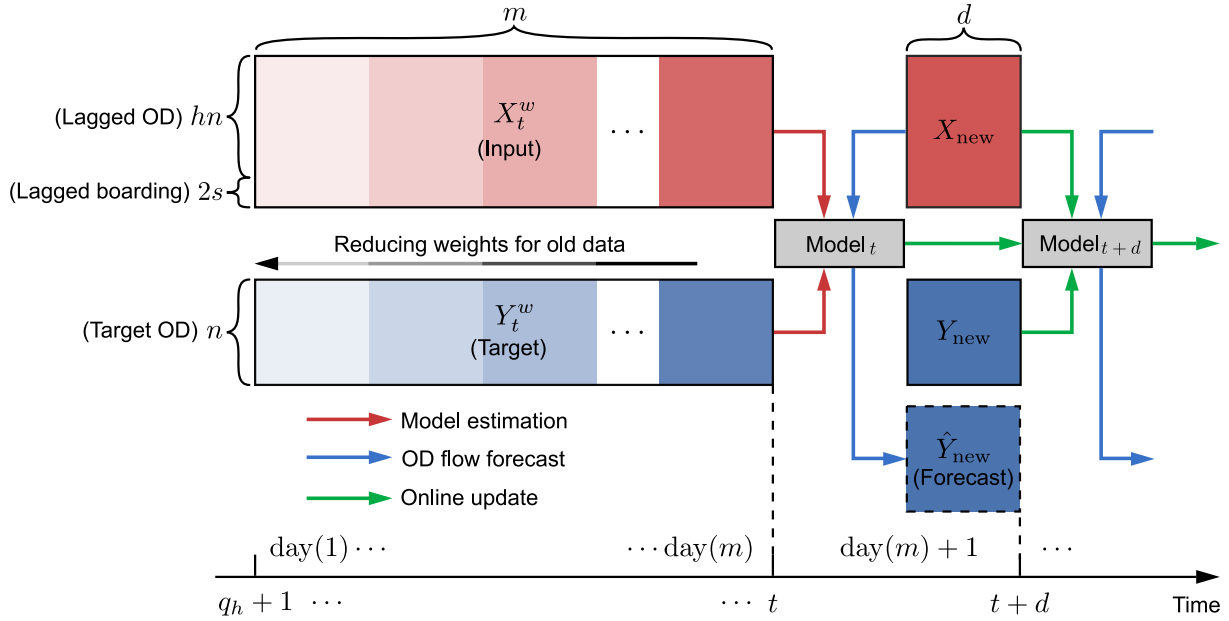


Figure 2: Model framework for HW-DMD. Model input X contains hn rows for lagged OD snapshots and $2s$ rows for lagged boarding snapshots. Columns in Y and \hat{Y} are respectively real and forecasted snapshots for OD flow. Model coefficients are estimated by weighted historical data (X_t^w and Y_t^w) and updated daily whenever new data come.

5.2. Model Estimation

We prefer a low-rank approximation of G_t over a full matrix of the optimal solution of Eq. (10). This is because storing the large full matrix is prohibitive, and the optimal solution often leads to overfitting problems, especially for the sparse and noisy OD data. Luckily, we can find a pretty good approximation thanks to the low-rank feature of OD data.

Similar to the exact DMD, we first compute the truncated SVD on the weighted augmented data matrix $X_t^w \approx U_X \Sigma_X V_X^\top$, where we keep r_X ($r_X \ll m$) largest singular values and $U_X \in \mathbb{R}^{(hn+2s) \times r_X}$, $\Sigma_X \in \mathbb{R}^{r_X \times r_X}$, $V_X \in \mathbb{R}^{m \times r_X}$. As shown in Fig. 1, a few leading singular values can well capture the entire data. Therefore, an approximation for coefficient matrices are

$$G_t = Y_t^w X_t^{w+} \approx Y_t^w V_X \Sigma_X^{-1} U_X^\top, \quad (11)$$

$$[A_{t,1}, \dots, A_{t,h}, A_{t,b1}, A_{t,b2}] \approx [Y_t^w V_X \Sigma_X^{-1} U_{X,1}^\top, \dots, Y_t^w V_X \Sigma_X^{-1} U_{X,h}^\top, Y_t^w V_X \Sigma_X^{-1} U_{X,b1}^\top, Y_t^w V_X \Sigma_X^{-1} U_{X,b2}^\top], \quad (12)$$

where $U_X^\top = [U_{X,1}^\top, \dots, U_{X,h}^\top, U_{X,b1}^\top, U_{X,b2}^\top]$, $U_{X,i}, \dots, U_{X,h} \in \mathbb{R}^{n \times r_X}$, and $U_{X,b1}, U_{X,b2} \in \mathbb{R}^{s \times r_X}$.

The results computed from Eq. (11) and Eq. (12) are still prohibitive. Therefore, for each column in Y_t^w , we seek a transformation $\mathbf{y}_i^w \rightarrow \tilde{\mathbf{y}}_i^w$ such that $\tilde{\mathbf{y}}_i^w \in \mathbb{R}^{r_Y}$ and $r_Y \ll n$. In doing so, we compute another rank- r_Y truncated SVD of the target matrix $Y_t^w \approx U_Y \Sigma_Y V_Y^\top$. The columns of U_Y form an orthonormal basis, the transformation $\tilde{\mathbf{y}}_i^w = U_Y^\top \mathbf{y}_i^w$ compute the coordinates of \mathbf{y}_i^w on this basis. The coefficient matrices in the reduced-order subspace (the column space of U_Y) can be approximated by

$$\tilde{A}_{t,i} = U_Y^\top A_{t,i} U_Y \approx U_Y^\top Y_t^w V_X \Sigma_X^{-1} U_{X,i}^\top U_Y \quad \forall i \in \{1, 2, \dots, h\}, \quad (13)$$

$$\tilde{A}_{t,bj} = U_Y^\top A_{t,bj} \approx U_Y^\top Y_t^w V_X \Sigma_X^{-1} U_{X,bj}^\top \quad \forall j \in \{1, 2\}, \quad (14)$$

where $\tilde{A}_{t,i} \in \mathbb{R}^{r_Y \times r_Y}$ and $\tilde{A}_{t,bj} \in \mathbb{R}^{r_Y \times s}$. Finally, we can write the model of Eq. (4) in the reduced-order subspace

$$\tilde{Y}_t \approx \tilde{A}_{t,1} \tilde{Y}_{t-q_1} + \tilde{A}_{t,2} \tilde{Y}_{t-q_2} + \dots + \tilde{A}_{t,h} \tilde{Y}_{t-q_h} + \tilde{A}_{t,b1} B_{t-1} + \tilde{A}_{t,b1} B_{t-2}, \quad (15)$$

where $\tilde{Y}_i = U_Y^\top Y_i$. The final forecast of an OD snapshot $\hat{\mathbf{y}}_i$ can be calculated by transforming back to the original basis by $\hat{\mathbf{y}}_i = U_Y \tilde{\mathbf{y}}_i$.

The forecast value $\hat{\mathbf{y}}_i$ of this model is restricted on the column space of U_Y , but it is a good approximation since the space is determined by leading singular vectors. The truncated SVD keeps most information and filters out noise and anomalies. The reduction in the parameter flexibility and data noise also address the overfitting problem. Most

importantly, with reduced coefficient matrices $\tilde{A}_{t,(\cdot)}$ and projection bases U_Y, U_X , we avoid calculating and storing the giant coefficient matrices $A_{t,(\cdot)}$. The major computational costs in model estimation is the SVD part. Current numerical software can solve large-scale SVD very efficiently. Therefore, estimating a HW-DMD model is very fast. We can further derive the eigenvalues and eigenvectors of coefficient matrices (Proctor et al., 2016). But this is not necessary because there is no clear physical meaning for eigenvectors in a high-order vector autoregression.

5.3. Online Update

A model trained by dated data may not reflect the recent dynamic in a system. Instead of retraining using entire data, we develop an online algorithm that updates HW-DMD daily with new observations without storing historical data, as shown in Fig. 2. Similar algorithms for online DMD have been developed by Hemati et al. (2014); Zhang et al. (2019a); Alfatlawi and Srivastava (2019). We extend the online DMD update algorithm to a high-order weighted version. Our algorithm inherits from the work by Hemati et al. (2014).

To illustrate the update algorithm, we need to reorganize Eq. (11)–(14). Let $\tilde{X}_i^w = U_X^\top X_i^w$ and $\tilde{Y}_i^w = U_Y^\top Y_i^w$ be the projection of data to the coordinates of U_X and U_Y , respectively. Using the fact $(U_X \tilde{X}_t^w)^+ = V_X \Sigma_X^{-1} U_X^\top$, we can rewrite Eq. (11) as

$$G_t \approx Y_t^w (U_X \tilde{X}_t^w)^+ \quad (16)$$

$$= Y_t^w \tilde{X}_t^{w\top} \left(\tilde{X}_t^w \tilde{X}_t^{w\top} \right)^+ U_X^\top. \quad (17)$$

Therefore, Eq. (13) and (14) becomes

$$\tilde{A}_{t,i} \approx \tilde{Y}_t^w \tilde{X}_t^{w\top} \left(\tilde{X}_t^w \tilde{X}_t^{w\top} \right)^+ U_{X,i}^\top U_Y = P Q_X^+ U_{X,i}^\top U_Y \quad \forall i \in \{1, \dots, h\}, \quad (18)$$

$$\tilde{A}_{t,bj} \approx \tilde{Y}_t^w \tilde{X}_t^{w\top} \left(\tilde{X}_t^w \tilde{X}_t^{w\top} \right)^+ U_{X,bj}^\top = P Q_X^+ U_{X,bj}^\top \quad \forall j \in \{1, 2\}. \quad (19)$$

Where $P = \tilde{Y}_t^w \tilde{X}_t^{w\top} \in \mathbb{R}^{r_Y \times r_X}$, $Q_X = \tilde{X}_t^w \tilde{X}_t^{w\top} \in \mathbb{R}^{r_X \times r_X}$. To facilitate the online update, we define an additional matrix $Q_Y = \tilde{Y}_t^w \tilde{Y}_t^{w\top} \in \mathbb{R}^{r_Y \times r_Y}$.

After the reorganization, model coefficients are represented by three ‘‘core’’ matrices P, Q_X, Q_Y and two projection matrices U_X, U_Y . Note these matrices are also time-varying. For simplicity, we omit the t subscript and regard they are always ‘‘up to date’’. Moreover, there are two important properties for the core matrices.

Property 1. *Given new observations $Y_{\text{new}} \in \mathbb{R}^{n \times d}$ and $X_{\text{new}} \in \mathbb{R}^{(hn+2s) \times d}$ from a new day, where d is the number of snapshots per day. Under the same projection matrices, the new core matrices can be updated by*

$$P \leftarrow \rho P + \tilde{Y}_{\text{new}} \tilde{X}_{\text{new}}^\top, \quad (20)$$

$$Q_X \leftarrow \rho Q_X + \tilde{X}_{\text{new}} \tilde{X}_{\text{new}}^\top, \quad (21)$$

$$Q_Y \leftarrow \rho Q_Y + \tilde{Y}_{\text{new}} \tilde{Y}_{\text{new}}^\top. \quad (22)$$

Where $\tilde{X}_{\text{new}} = U_X^\top X_{\text{new}}$, $\tilde{Y}_{\text{new}} = U_Y^\top Y_{\text{new}}$.

Property 2. *Denote $\bar{Y}_t^w = U_Y \tilde{Y}_t^w$ to be the recovered data from the reduced data. If \mathbf{v}_i is the i -th eigenvector of Q_Y , then $U_Y \mathbf{v}_i$ is the i -th left singular vector of \bar{Y}_t^w . The same property applies to Q_X and $\bar{X}_t^w = U_X \tilde{X}_t^w$.*

The proofs for these properties are shown in Appendix A. Property 1 is used to update the core matrices in a memory-saving way. Property 2 indicates we can use the eigenvectors of Q_Y to approximate the left singular vectors of Y_t^w (because $Y_t^w \approx \bar{Y}_t^w$), which is crucial for updating the projection matrices. Based on these properties, we summarize the online update algorithm in the following three steps.

1. **Expand projection matrices.** Let $E_Y = Y_{\text{new}} - U_Y U_Y^\top Y_{\text{new}}$ and $E_X = X_{\text{new}} - U_X U_X^\top X_{\text{new}}$ be the residuals that cannot be represented by the column space of U_X and U_Y . To incorporate these residuals, we expand projection matrices by $U_X \leftarrow [U_X, U_{E_X}]$ and $U_Y \leftarrow [U_Y, U_{E_Y}]$, where U_{E_X} and U_{E_Y} are the orthonormal bases (obtained by SVD or QR factorization) of E_X and E_Y , respectively.
2. **Update core matrices.** To align dimensions, we first pad P, Q_X , and Q_Y with zeros on the dimensions where U_X and U_Y expanded. Then update core matrices by Eq. (20)–(22).

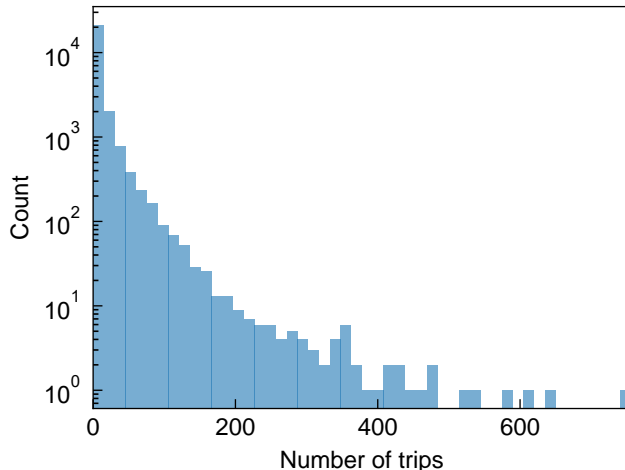


Figure 3: The histogram of $o_{i,j}$ in an OD snapshot of a morning peak.

3. **Compression.** The first two steps incorporate all new information at the cost of expanding dimensions. Next, we compress the model based on property 2. Denote V_X and V_Y to be matrices composed by the leading r_X and r_Y eigenvectors of Q_X and Q_Y , respectively. We can compress projection matrices by $U_X \leftarrow U_X V_X$, $U_Y \leftarrow U_Y V_Y$ to keep the leading singular vectors of \tilde{X}_{t+d}^w and \tilde{Y}_{t+d}^w . The core matrices can be compressed accordingly by $Q_X \leftarrow V_X^\top Q_X V_X$, $Q_Y \leftarrow V_Y^\top Q_Y V_Y$, $P \leftarrow V_Y^\top P V_X$.

Besides the daily update, a more general setting can be updating the model every k intervals or only doing the compression step when r_X or r_Y exceeds a threshold. This paper adopts the daily update described above because metro systems often have a one-day periodicity. In terms of computational efficiency, the online update algorithm computes SVD for d -column data matrices and eigenvalue decomposition of Q_X and Q_Y . The computation has a constant cost every day and is significantly faster than retraining using entire data. In terms of memory efficiency, historical data are not required when updating the model. All we need to store are three “core” matrices and two projection matrices. Regarding the error, the online algorithm does not take into account the previously truncated part. This impact is negligible because the truncated part is mostly noise, and old data are forgotten exponentially. Our experiments in section 6.5 show the online algorithm performs pretty close to or even slightly better than retraining.

6. Experiments

In this section, we compare the proposed HW-DMD with other forecasting models by real-world data. We begin with an introduction to data and experimental settings. Next, we compare models’ performances by OD matrices and the boarding flow derived from the OD matrices. Finally, we examine the long-term effect of the online HW-DMD update algorithm.

6.1. Data and experimental settings

We examine our model with the metro smart card data from Guangzhou, China. Our data cover around 301 million trips among 159 metro stations in Guangzhou from July 1st to September 30th, 2017. The smart card data records the origin, destination, and the entry and exit time of each metro trip. Guangzhou metro operates from 6:00 to 24:00. We aggregate OD snapshots by a 30-minute time interval, which means 36 snapshots per day and $159 \times 159 = 25281$ elements per snapshot. Note that too small an interval may result in too sparse OD matrices; we choose the 30-minute interval to balance the practical and model requirements. Fig. 3 further shows the distribution of $o_{i,j}$ from an OD snapshot of a typical morning peak. The distribution roughly follows a power law, with most OD pairs have small volumes while a few of them are significantly larger. The highly skewed distribution is hard to be properly handled by conventional forecast models.

Our experiment only focuses on the forecast of workdays, and Friday is connected to the next Monday. We use the first twenty weekdays (July 3rd to July 28th) as the training set, the next ten weekdays (July 31st to August 11th) as the validation set, and the next ten weekdays (August 14th to August 25th) as the test set. All models’ hyper-parameters are tuned based on the validation set, and their performances are compared on the test set. There are

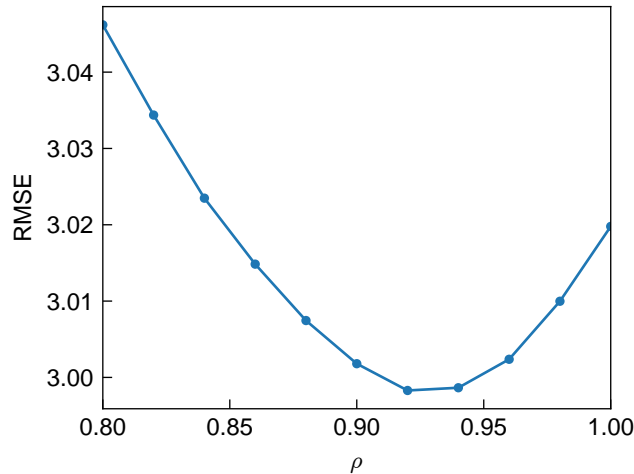


Figure 4: The effect of ρ to the forecast OD RMSE in the validation set.

additional one-month data after the test set; we use these data to study the long-term effect of the online HW-DMD update algorithm.

The performance of a model is evaluated by the root mean square error (RMSE), the weighted mean absolute percentage error (WMAPE), and the coefficient of determination (denoted as R^2):

$$\text{RMSE}(\alpha, \hat{\alpha}) = \sqrt{\frac{1}{N} \sum_{i=1}^N (\alpha_i - \hat{\alpha}_i)^2},$$

$$\text{WMAPE}(\alpha, \hat{\alpha}) = \frac{\sum_{i=1}^N |\alpha_i - \hat{\alpha}_i|}{\sum_{i=1}^N |\alpha_i|} \times 100\%,$$

$$R^2(\alpha, \hat{\alpha}) = 1 - \frac{\sum_{i=1}^N (\alpha_i - \hat{\alpha}_i)^2}{\sum_{i=1}^N (\alpha_i - \bar{\alpha})^2}.$$

Where α and $\hat{\alpha}$ are respectively the real and predicted values; $\bar{\alpha}$ is the average value of α ; N is the total number of elements under different time intervals and locations. The three performance metrics are computed for both OD flow o and boarding flow b (forecasted by $\hat{b}_{t,i} = \sum_j \hat{o}_{t,i,j}$).

6.2. Hyper-parameters

We use the online update algorithm for HW-DMD if not otherwise specified. Hyper-parameters for HW-DMD include time lags q_1, \dots, q_h , the SVD truncation rank r_X, r_Y , and the forgetting ratio ρ . We determine these parameters in an sequential order.

We first set $r_X = r_Y = 100$ and $\rho = 1$ and select time lags in a greedy manner. For time lags within one day ($3 \leq q_i \leq 36$), we repeatedly add a “currently best” time lag based on the RMSE of the validation set until a new lag brings no improvement or the number of lags reaches ten. This procedure selects $\{3, 4, 8, 14, 19, 28, 30, 33, 35, 36\}$ as time lags. The considerable high-order time lags in the result indicate long-term auto-correlations of OD time series. For example, the lag 19 roughly equals a typical work duration (9.5 hours). A study by [Cheng et al. \(2020\)](#) showed a strong correlation between the departure trips for commuters in the morning and the returning trips in the afternoon. The metro OD flow is also highly regular; the largest several lags (e.g., 33, 35, and 36) capture the one-day periodicity.

Next, we determine r_X and r_Y by a grid search from 20 to 100 at an interval of 10. The best r_Y is 50. A larger r_X than 100 still brings a marginal improvement, but we truncate r_X at 100 to restrict the model size (r_X affects the size of U_X in the online update). Lastly, we set ρ to be 0.92 based on a line search from 0.8 to 1. As shown in Fig. 4, we can see assigning smaller weights for old data indeed improves the forecast. Because $0.92^8 \approx 0.51$, using $\rho = 0.92$ is roughly equivalent to halving the weight every eight days.

6.3. Benchmark models

We compare HW-DMD with the following benchmark models:

- HA: Historical Average. For the OD flow at a certain period (e.g., 7:00–7:30) of the day, HA uses the average OD flow at that period in the training set as the forecast value.
- TRMF: Temporal Regularized Matrix Factorization (Yu et al., 2016). TRMF is a matrix factorization model that imposes autoregression (AR) processes on each temporal factor. We use time lags $[1, \dots, 10]$ for the AR processes. We set the number of factors to be 45 based on the parameter tuning.
- ConvLSTM: Convolutional LSTM (Shi et al., 2015). It is a deep recurrent neural network model that forecasts future frames of matrix time series (e.g., videos). Here we use it to forecast future OD matrices by the most recent ten OD matrices. We apply a three-layer LSTM structure with respectively 8, 8, and 1 filters. We set the kernel size to be 3×3 for all convolutional layers in the model.
- FNN: A two-layer Feedforward Neural Network. We use the OD snapshots of 3-10 lags ago and the boarding flow snapshot of 1-2 lags ago as the input features. Based on parameter tuning, we set the hidden layer’s size to be 60 and use a linear activation.
- SARIMA: Seasonal Auto-Regressive Integrated Moving Average. We only use SARIMA to forecast the boarding flow since SARIMA only handles one-dimensional time series. We use the order ARIMA(2, 0, 1)(1, 1, 0)[36] for all the stations and fit 159 separate models. This model configuration is the same as Cheng et al. (2020) and was tested to be suitable for most metro stations.

Applying TRMF, ConvLSTM, and FNN to the original data (or after a normalization) can hardly obtain a forecast better than HA. This phenomenon was also found by Gong et al. (2018, 2020). This is because the OD data are high-dimensional, sparse, noisy, and highly skewed. To improve the forecast of these models, we apply TRMF, ConvLSTM, and FNN to the residuals after subtracting the HA from the original data. This “mean-removal” processing also weakens the data’s periodicity; therefore, we do not use seasonal lags in these models. Besides, because the standard TRMF and ConvLSTM cannot use the boarding flow as extra inputs, we ignore the delayed data availability problem for these models and assume all historical OD snapshots are available.

6.4. Forecast result

We apply trained models to the test set and forecast OD matrices of the next three steps at each time interval. Note OD snapshots of 1-2 lags ago are unknown; they are replaced by previously forecasted OD snapshots when doing multi-step rolling forecasting by HW-DMD/FNN. Next, the boarding flow can be calculated from OD matrices. We compare the forecast accuracy of models in terms of OD flow and boarding flow.

Table 1 shows the results of OD flow forecast. We can see HW-DMD outperforms other models in all evaluation metrics. Even the three-step forecast of HW-DMD is better than the one-step forecast of other models. Although TRMF, FNN, and ConvLSTM are trained on the residuals after subtracting the HA from the original data, the improvement of these models compared with HA is limited. In contrast, HW-DMD is directly applied to the original data but provides a significantly better forecast, demonstrating its strong prediction power in handling the sparse, noisy, and high-dimensional OD data.

Table 1: Models’ performance for OD flow forecasting.

| | | HW-DMD | TRMF | FNN | Conv-LSTM | HA |
|------------|-------|---------------|--------|--------|-----------|--------|
| One-step | RMSE | 3.05 | 3.25 | 3.26 | 3.38 | 3.43 |
| | WMAPE | 29.65% | 30.98% | 30.95% | 30.85% | 31.21% |
| | R^2 | 0.957 | 0.951 | 0.951 | 0.947 | 0.945 |
| Two-step | RMSE | 3.09 | 3.32 | 3.27 | 3.39 | 3.43 |
| | WMAPE | 29.77% | 31.35% | 31.00% | 30.96% | 31.21% |
| | R^2 | 0.956 | 0.949 | 0.950 | 0.946 | 0.945 |
| Three-step | RMSE | 3.11 | 3.37 | 3.29 | 3.40 | 3.43 |
| | WMAPE | 29.79% | 31.68% | 31.02% | 31.04% | 31.21% |
| | R^2 | 0.955 | 0.947 | 0.950 | 0.946 | 0.945 |

Examining the aggregated boarding flow is important because it reflects if the forecast errors in OD matrices’ are properly distributed, which is crucial when using OD matrices in traffic assignments. Moreover, the boarding flow

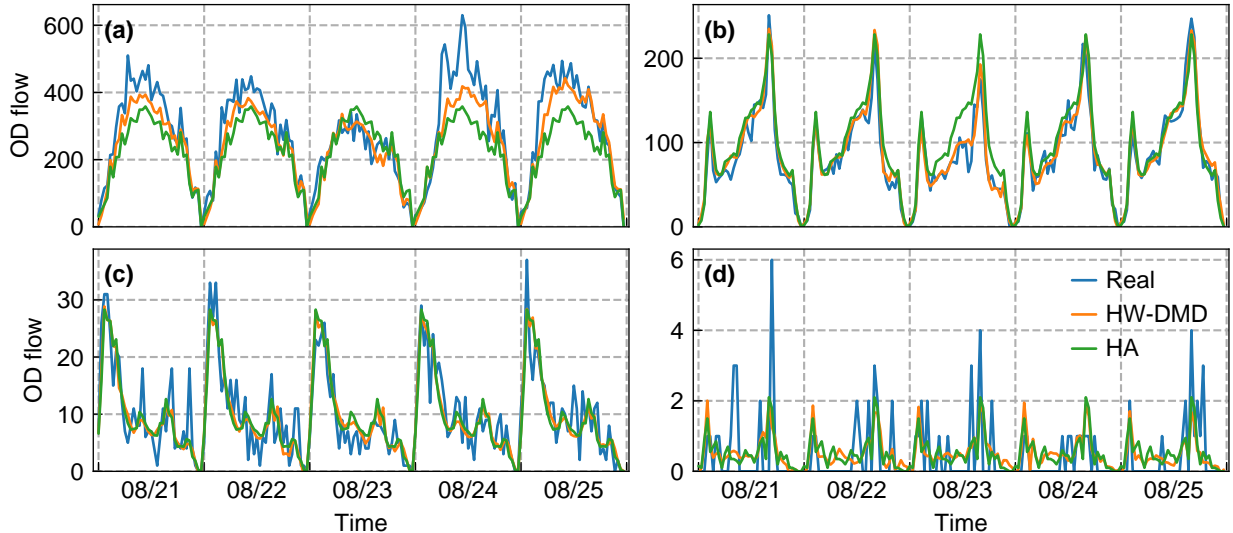


Figure 5: The real and forecasted time series of four selected OD pairs. (a) to (d) are in a flow decreasing order.

itself is of interest to many applications. Table 2 shows the boarding flow forecasting; all models except SARIMA calculate boarding flow by OD matrices. HW-DMD is still the best among all models. Particularly, HW-DMD significantly outperforms SARIMA, a well-established boarding flow forecasting model, indicating the advantage of OD-matrices-based boarding flow forecasting.

Table 2: Models' performance for boarding flow forecasting.

| | | HW-DMD | TRMF | FNN | Conv-LSTM | HA | SARIMA |
|------------|-------|---------------|--------|--------------|-----------|--------|--------|
| One-step | RMSE | 93.99 | 108.78 | 106.44 | 123.26 | 136.56 | 110.23 |
| | WMAPE | 6.09% | 6.99% | 6.74% | 7.35% | 8.38% | 7.15% |
| | R^2 | 0.991 | 0.987 | 0.988 | 0.984 | 0.980 | 0.987 |
| Two-step | RMSE | 102.61 | 116.40 | 108.75 | 128.11 | 136.56 | 120.60 |
| | WMAPE | 6.68% | 7.52% | 6.89% | 7.78% | 8.38% | 7.65% |
| | R^2 | 0.989 | 0.986 | 0.988 | 0.983 | 0.980 | 0.985 |
| Three-step | RMSE | 107.58 | 122.52 | 110.25 | 130.75 | 136.56 | 126.52 |
| | WMAPE | 6.98% | 7.95% | 6.98% | 7.98% | 8.38% | 7.93% |
| | R^2 | 0.988 | 0.984 | 0.987 | 0.982 | 0.980 | 0.983 |

Fig. 5 shows the real and one-step forecast of OD flow at four representative OD pairs. The OD flow exhibits a clear daily periodicity, explaining why HA already works reasonably well. HW-DMD is much better at forecasting the fluctuation of high-volume OD flow, as shown in Fig. 5 (a) and (b). In Fig. 5 (a), the forecast of HW-DMD is often lower than the real value; this is hard to avoid since there is a two-lag delay when collecting the real OD flow. More OD pairs in the system are like Fig. 5 (c) and (d) with a low flow but high noise. Under such high volatility, the forecast by HW-DMD is similar to HA. In fact, the performances of other models are often undermined by noise. The SVD truncation to the data greatly enhances HW-DMD's ability in handling the noise data (Fig. 1). Overall, HW-DMD achieves a great balance between forecasting and noise reduction, which is particularly hard for such a high dimensional system with diverse flow magnitude.

6.5. Effect of the online update

The online update algorithm proposed in section 5.3 can update HW-DMD's parameters daily without storing historical data. We particularly care about if errors will accumulate if keep using this algorithm for a long time. Therefore, we apply the online update algorithm to all the two-month data after the training set to evaluate its long-term effect. In comparison, we retrain two HW-DMD models (with $\rho=0.92$ and 1 respectively) every day using all historical data up until the latest. The results are shown in Fig. 6. We summarize the key findings for Fig. 6 as follows:

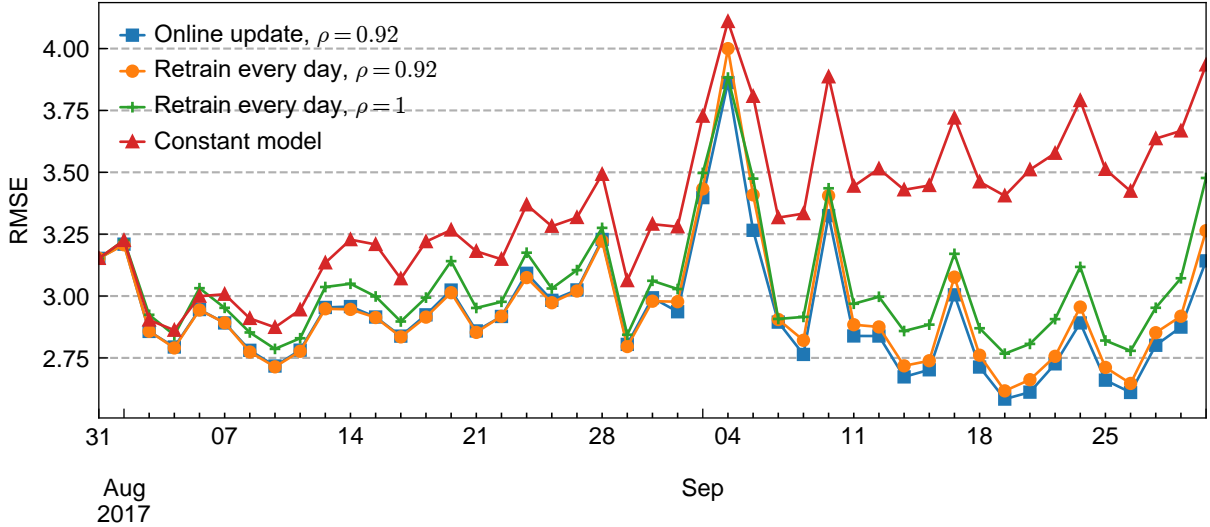


Figure 6: The evolution of forecast RMSE under different HW-DMD update methods. Each marker represents the RMSE of forecasted OD flow during a day. Numbered dates in the horizontal axis are Mondays; weekends are skipped.

- The RMSE of a constant model gradually increases over time. This indicates the metro system’s dynamics are time-evolving; thus, forecast models should be updated/retrained regularly for better performance.
- The RMSE curve of the online update algorithm clings to the model ($\rho = 0.92$) retrained every day by entire historical data, showing the online HW-DMD update algorithm works consistently well in long-term applications. For a large training set (e.g., after September in Fig. 6), the online update approach even performs slightly better than retraining.
- Properly reducing the weight for old data improves the forecast. Compare $\rho = 0.92$ with $\rho = 1$ for the two retrained models; the benefits of forgetting the old data become more significant as the training data increases.
- The OD flow of certain weekdays can be harder to forecast. Especially for the forecast of September. The RMSEs on Fridays are significantly higher than other weekdays.

Many forecast models do not consider the time-evolving dynamics of a metro system. A regular retrain can be prohibitive, especially for complicated models (e.g., deep learning models). This experiment shows the online update algorithm for HW-DMD is a memory-saving and accurate approach to keep an HW-DMD model up to date.

7. Conclusions and discussion

This paper proposes a high-order weighted dynamic mode decomposition (HW-DMD) model to solve the real-time short-term OD matrices forecast problem in metro systems. Experiments show the HW-DMD significantly outperforms common forecast models under the high-dimensional, sparse, noisy, and skewed OD data. Particularly, we address the delayed data availability problem and the time-evolving dynamics of metro systems, which are often ignored in the literature. The idea of the forgetting rate and online update in dealing with a time-evolving system is also beneficial for other forecasting models. Moreover, the implementation of HW-DMD is simple, and the computation is very efficient. We welcome the use of HW-DMD in forecasting general high-dimensional data.

We discuss several future research directions. (1) Current HW-DMD reshapes OD matrices into vectors for dimensionality reduction. However, performing dimensionality reduction directly on OD matrices may better utilize the column/row-wise correlations and produce more concise models (Chen et al., 2020; Gong et al., 2020). A difficulty in this direction is that the low-rank feature in metro OD matrices is relatively weak. Because the diagonal elements of metro OD matrices are all zeros. (2) Another future direction is to use a non-linear model instead of the current linear model in the reduced space, such as the deep factor forecast model (Wang et al., 2019a). But a limitation for a non-linear model is that an online update method may be hard to derive or impossible. (3) Lastly, current HW-DMD uses external features, such as the boarding flow, simply as covariates. Incorporating more general features (e.g., weather, events) and network structure to improve the HW-DMD is worth investigating.

Acknowledgement

This research is supported by the Natural Sciences and Engineering Research Council (NSERC) of Canada, Mitacs, [exo.quebec](https://exo.quebec/en) (<https://exo.quebec/en>), and the Canada Foundation for Innovation (CFI). The code for HW-DMD is available at <https://github.com/chengzhanhong/HW-DMD>.

References

- Alfatlawi, M., Srivastava, V., 2019. An incremental approach to online dynamic mode decomposition for time-varying systems with applications to eeg data modeling. arXiv preprint arXiv:1908.01047.
- Arbabi, H., Mezic, I., 2017. Ergodic theory, dynamic mode decomposition, and computation of spectral properties of the koopman operator. *SIAM Journal on Applied Dynamical Systems* 16 (4), 2096–2126.
- Avila, A., Mezić, I., 2020. Data-driven analysis and forecasting of highway traffic dynamics. *Nature communications* 11 (1), 1–16.
- Brunton, S. L., Brunton, B. W., Proctor, J. L., Kaiser, E., Kutz, J. N., 2017. Chaos as an intermittently forced linear system. *Nature communications* 8 (1), 1–9.
- Chen, E., Ye, Z., Wang, C., Xu, M., 2019. Subway passenger flow prediction for special events using smart card data. *IEEE Transactions on Intelligent Transportation Systems* 21 (3), 1109–1120.
- Chen, R., Xiao, H., Yang, D., 2020. Autoregressive models for matrix-valued time series. *Journal of Econometrics*.
- Cheng, Z., Trepanier, M., Sun, L., 2020. Incorporating travel behavior regularity into passenger flow forecasting. arXiv preprint arXiv:2004.00992.
- Chu, K.-F., Lam, A. Y., Li, V. O., 2019. Deep multi-scale convolutional lstm network for travel demand and origin-destination predictions. *IEEE Transactions on Intelligent Transportation Systems*.
- Dai, X., Sun, L., Xu, Y., 2018. Short-term origin-destination based metro flow prediction with probabilistic model selection approach. *Journal of Advanced Transportation* 2018.
- Gong, Y., Li, Z., Zhang, J., Liu, W., Zheng, Y., 2020. Online spatio-temporal crowd flow distribution prediction for complex metro system. *IEEE Transactions on Knowledge and Data Engineering*.
- Gong, Y., Li, Z., Zhang, J., Liu, W., Zheng, Y., Kirsch, C., 2018. Network-wide crowd flow prediction of sydney trains via customized online non-negative matrix factorization. In: *Proceedings of the 27th ACM International Conference on Information and Knowledge Management*. pp. 1243–1252.
- Hemati, M. S., Williams, M. O., Rowley, C. W., 2014. Dynamic mode decomposition for large and streaming datasets. *Physics of Fluids* 26 (11), 111701.
- Hu, J., Yang, B., Guo, C., Jensen, C. S., Xiong, H., 2020. Stochastic origin-destination matrix forecasting using dual-stage graph convolutional, recurrent neural networks. In: *2020 IEEE 36th International Conference on Data Engineering (ICDE)*. IEEE, pp. 1417–1428.
- Ke, J., Qin, X., Yang, H., Zheng, Z., Zhu, Z., Ye, J., 2021. Predicting origin-destination ride-sourcing demand with a spatio-temporal encoder-decoder residual multi-graph convolutional network. *Transportation Research Part C: Emerging Technologies* 122, 102858.
- Kwak, S., Geroliminis, N., 2020. Travel time prediction for congested freeways with a dynamic linear model. *IEEE Transactions on Intelligent Transportation Systems*.
- Li, Y., Wang, X., Sun, S., Ma, X., Lu, G., 2017. Forecasting short-term subway passenger flow under special events scenarios using multiscale radial basis function networks. *Transportation Research Part C: Emerging Technologies* 77, 306–328.
- Liu, J., Zheng, F., van Zuylen, H. J., Li, J., 2020. A dynamic od prediction approach for urban networks based on automatic number plate recognition data. *Transportation Research Procedia* 47, 601–608.

- Liu, L., Qiu, Z., Li, G., Wang, Q., Ouyang, W., Lin, L., 2019a. Contextualized spatial-temporal network for taxi origin-destination demand prediction. *IEEE Transactions on Intelligent Transportation Systems* 20 (10), 3875–3887.
- Liu, Y., Liu, Z., Jia, R., 2019b. Deepfpf: A deep learning based architecture for metro passenger flow prediction. *Transportation Research Part C: Emerging Technologies* 101, 18–34.
- Proctor, J. L., Brunton, S. L., Kutz, J. N., 2016. Dynamic mode decomposition with control. *SIAM Journal on Applied Dynamical Systems* 15 (1), 142–161.
- Ren, J., Xie, Q., 2017. Efficient od trip matrix prediction based on tensor decomposition. In: 2017 18th IEEE International Conference on Mobile Data Management (MDM). IEEE, pp. 180–185.
- Rowley, C. W., Mezić, I., Bagheri, S., Schlatter, P., Henningson, D., et al., 2009. Spectral analysis of nonlinear flows. *Journal of fluid mechanics* 641 (1), 115–127.
- Schmid, P. J., 2010. Dynamic mode decomposition of numerical and experimental data. *Journal of fluid mechanics* 656, 5–28.
- Shen, L., Shao, Z., Yu, Y., Chen, X., 2020. Hybrid approach combining modified gravity model and deep learning for short-term forecasting of metro transit passenger flows. *Transportation Research Record*, 0361198120968823.
- Shi, X., Chen, Z., Wang, H., Yeung, D.-Y., Wong, W.-K., Woo, W.-c., 2015. Convolutional lstm network: A machine learning approach for precipitation nowcasting. *Advances in neural information processing systems* 28, 802–810.
- Sun, Y., Leng, B., Guan, W., 2015. A novel wavelet-svm short-time passenger flow prediction in beijing subway system. *Neurocomputing* 166, 109–121.
- Toqué, F., Côme, E., El Mahrsi, M. K., Oukhellou, L., 2016. Forecasting dynamic public transport origin-destination matrices with long-short term memory recurrent neural networks. In: 2016 IEEE 19th international conference on intelligent transportation systems (ITSC). IEEE, pp. 1071–1076.
- Tu, J. H., Rowley, C. W., Luchtenburg, D. M., Brunton, S. L., Kutz, J. N., 2014. On dynamic mode decomposition: Theory and applications. *Journal of Computational Dynamics* 1 (2), 391–421.
- Wang, S., Miao, H., Chen, H., Huang, Z., 2020. Multi-task adversarial spatial-temporal networks for crowd flow prediction. In: *Proceedings of the 29th ACM International Conference on Information & Knowledge Management*. pp. 1555–1564.
- Wang, Y., Smola, A., Maddix, D. C., Gasthaus, J., Foster, D., Januschowski, T., 2019a. Deep factors for forecasting. *arXiv preprint arXiv:1905.12417*.
- Wang, Y., Yin, H., Chen, H., Wo, T., Xu, J., Zheng, K., 2019b. Origin-destination matrix prediction via graph convolution: a new perspective of passenger demand modeling. In: *Proceedings of the 25th ACM SIGKDD International Conference on Knowledge Discovery & Data Mining*. pp. 1227–1235.
- Wei, Y., Chen, M.-C., 2012. Forecasting the short-term metro passenger flow with empirical mode decomposition and neural networks. *Transportation Research Part C: Emerging Technologies* 21 (1), 148–162.
- Xiong, X., Ozbay, K., Jin, L., Feng, C., 2020. Dynamic origin-destination matrix prediction with line graph neural networks and kalman filter. *Transportation Research Record* 2674 (8), 491–503.
- Yu, H.-F., Rao, N., Dhillon, I. S., 2016. Temporal regularized matrix factorization for high-dimensional time series prediction. In: *Advances in neural information processing systems*. pp. 847–855.
- Yu, Y., Zhang, Y., Qian, S., Wang, S., Hu, Y., Yin, B., 2020. A low rank dynamic mode decomposition model for short-term traffic flow prediction. *IEEE Transactions on Intelligent Transportation Systems*.
- Zhang, D., Xiao, F., Shen, M., Zhong, S., 2021. DNEAT: A novel dynamic node-edge attention network for origin-destination demand prediction. *Transportation Research Part C: Emerging Technologies* 122, 102851.
- Zhang, H., Rowley, C. W., Deem, E. A., Cattafesta, L. N., 2019a. Online dynamic mode decomposition for time-varying systems. *SIAM Journal on Applied Dynamical Systems* 18 (3), 1586–1609.

Zhang, J., Che, H., Chen, F., Mae, W., He, Z., 2020a. Short-term prediction of urban rail transit origin-destination flow: A channel-wise attentive split-convolutional neural network method. arXiv preprint arXiv:2008.08036.

Zhang, J., Chen, F., Cui, Z., Guo, Y., Zhu, Y., 2020b. Deep learning architecture for short-term passenger flow forecasting in urban rail transit. IEEE Transactions on Intelligent Transportation Systems.

Zhang, J., Chen, F., Wang, Z., Liu, H., 2019b. Short-term origin-destination forecasting in urban rail transit based on attraction degree. IEEE Access 7, 133452–133462.

Appendix A. Proof for properties

Proof of property 1

Proof. Given new observations $Y_{\text{new}} \in \mathbb{R}^{n \times d}$ and $X_{\text{new}} \in \mathbb{R}^{(hn+2s) \times d}$ from a new day, Under the same projection matrices, the new core matrix P can be computed by

$$\tilde{Y}_{t+d}^w \tilde{X}_{t+d}^{w\top} = [\sigma \tilde{Y}_t^w, U_Y^\top Y_{\text{new}}][\sigma \tilde{X}_t^w, U_X^\top X_{\text{new}}]^\top \quad (\text{A.1})$$

$$= [\sigma \tilde{Y}_t^w, \tilde{Y}_{\text{new}}][\sigma \tilde{X}_t^w, \tilde{X}_{\text{new}}]^\top \quad (\text{A.2})$$

$$= \sigma^2 \tilde{Y}_t^w \tilde{X}_t^{w\top} + \tilde{Y}_{\text{new}} \tilde{X}_{\text{new}}^\top \quad (\text{A.3})$$

$$= \rho P + \tilde{Y}_{\text{new}} \tilde{X}_{\text{new}}^\top. \quad (\text{A.4})$$

Therefore, P can be updated by $P \leftarrow \rho P + \tilde{Y}_{\text{new}} \tilde{X}_{\text{new}}^\top$. Similar proof applies to Q_X and Q_Y . \square

Proof of property 2

Proof. Compute SVD $\tilde{Y}_t^w = \bar{U} \bar{\Sigma} \bar{V}^\top$, then

$$\tilde{Y}_t^w \tilde{Y}_t^{w\top} = \bar{U} \bar{\Sigma} \bar{V}^\top \bar{V} \bar{\Sigma}^\top \bar{U}^\top = \bar{U} (\bar{\Sigma} \bar{\Sigma}) \bar{U}^\top, \quad (\text{A.5})$$

$$(\tilde{Y}_t^w \tilde{Y}_t^{w\top}) \bar{U} = \bar{U} (\bar{\Sigma} \bar{\Sigma}) = \bar{U} \bar{\Lambda}. \quad (\text{A.6})$$

Therefore, columns of \bar{U} are the eigenvectors of $\tilde{Y}_t^w \tilde{Y}_t^{w\top}$ and the left singular vectors of \tilde{Y}_t^w . Substitute $\tilde{Y}_t^w \tilde{Y}_t^{w\top} = U_Y Q_Y U_Y^\top$ to Eq. (A.6), we have

$$(U_Y Q_Y U_Y^\top) \bar{U} = \bar{U} \bar{\Lambda}, \quad (\text{A.7})$$

$$Q_Y (U_Y^\top \bar{U}) = (U_Y^\top \bar{U}) \bar{\Lambda}. \quad (\text{A.8})$$

Define $V = U_Y^\top \bar{U}$. Then, each column \mathbf{v}_i in V is a eigenvector for Q_Y and $U_Y \mathbf{v}_i = U_Y (U_Y^\top \bar{\mathbf{u}}_i) = \mathbf{u}_i$ is a singular vector of \tilde{Y}_t^w . \square